Author Manuscript

Activated Intestinal Muscle Cells Promote Preadipocyte Migration: A Novel Mechanism for Creeping Fat Formation in Crohn's Disease

Ren Mao[1,2], **Genevieve Doyon**[2,3], **Ilyssa O. Gordon**[4], **Jian-Nan Li**[2], **Si-Nan Lin**[2], **Jie Wang**[2], **Thi Hong Nga Le**[2], **Michael Elias**[2], **Satya Kurada**[2,5], **Brian D. Southern**[2], **Mitchell Olman**[2], **Min-hu Chen**[1], **Shuai Zhao**[2], **Dina Dejanovic**[2], **Jyotsna Chandra**[2], **Pranab K. Mukherjee**[2], **Gail West**[2], **David R. van Wagoner**[6], **Claudio Fiocchi**[2,5], **Florian Rieder**[2,5]

[1]Department of Gastroenterology, First Affiliated Hospital of Sun Yat-sen University, Guangzhou, China

[2]Department of Inflammation and Immunity, Lerner Research Institute, Cleveland Clinic Foundation, Cleveland, Ohio, USA

[3]Aging Institute, University of Pittsburgh, Pittsburgh, Pennsylvania, USA

[4]Department of Pathology, Robert J. Tomsich Pathology and Laboratory Medicine Institute, Cleveland Clinic Foundation, Cleveland, USA

[5]Department of Gastroenterology, Hepatology and Nutrition, Digestive Diseases and Surgery Institute; Cleveland Clinic Foundation, Cleveland, USA

[6]Department of Cardiovascular and Metabolic Science, Lerner Research Institute, Cleveland Clinic Foundation, Cleveland, Ohio, USA

Abstract

Objective: Creeping fat, the wrapping of mesenteric fat around the bowel wall, is a typical feature of Crohn's disease, and is associated with stricture formation and bowel obstruction. How creeping fat forms is unknown, and we interrogated potential mechanisms using novel intestinal tissue and cell interaction systems.

Design: Tissues from normal, ulcerative colitis, non-strictured and strictured Crohn's disease intestinal specimens were obtained. The muscularis propria matrisome was determined via proteomics. Mesenteric fat explants, primary human pre-adipocytes and adipocytes were used in multiple *ex vivo* and *in vitro* cell migration systems on muscularis propria muscle cell derived or native extracellular matrix. Functional experiments included integrin characterization via flow cytometry and their inhibition with specific blocking antibodies and chemicals.

Results: Crohn's disease muscularis propria cells produced an extracellular matrix scaffold which is in direct spatial and functional contact with the immediately overlaid creeping fat. The scaffold contained multiple proteins, but only fibronectin production was singularly upregulated by TGF-β1. The muscle cell-derived matrix triggered migration of pre-adipocytes out of mesenteric fat, fibronectin being the dominant factor responsible for their migration. Blockade of α5β1 on the pre-adipocyte surface inhibited their migration out of mesenteric fat and on 3D decellularized intestinal tissue extracellular matrix.

Conclusion: Crohn's disease creeping fat appears to result from the migration of pre-adipocytes out of mesenteric fat and differentiation into adipocytes in response to an increased production of fibronectin by activated muscularis propria cells. These new mechanistic insights may lead to novel approaches for prevention of creeping fat-associated stricture formation.

Keywords

Crohn's disease; creeping fat; muscularis propria; extracellular matrix; fibronectin

INTRODUCTION

More than half of Crohn's disease (CD) patients develop fibrotic stricture-induced intestinal obstruction, and surgical intervention is necessary in approximately 80% of them[1, 2]. Despite increasingly potent anti-inflammatory therapy[1], incidence of strictures in CD has decreased only minimally and there are still no specific anti-fibrotic therapies.

While once recognized only as energy storage, fat tissue is now considered an endocrine organ with multiple functions[3]. Creeping fat (CF) is a distinctive body-weight independent accumulation of mesenteric fat wrapped around intestinal segments affected by CD[4, 5]. CF comprises dystrophic adipocytes, pre-adipocytes and inflammatory cells, is characterized by a distinct gene expression profile[4, 6], and appears almost exclusively at sites where there is muscularis propria (MP) hyperplasia and a fibrotic stricture[5, 7]. At these sites the pro-fibrotic transforming growth factor (TGF)-β1 is upregulated, which activates MP cells to produce excessive amounts of extracellular matrix (ECM)[8], and promotes the MP hyperplasia, now considered the main contributor to bowel wall thickening and luminal narrowing[9].

While CF was originally described almost a century ago[10] information on its mechanisms are surprisingly scant, because of lack of an animal model of CF and limited access to primary human intestinal cells. A recent very elegant investigation suggested that translocation of gut microbiota into the mesentery may drive formation of CF[6]. It seems reasonable to assume that CF and the adjacent MP are co-involved in the formation of

strictures [5], making their cellular components directly pertinent to the mechanisms of stricture formation. If these mechanisms are identified, CF development could be prevented and exploited for the treatment of stenosis-suffering CD patients.

In the absence of CF animal models, we carefully studied the CF-MP interface using unique primary human intestinal cells and tissues as well as novel cell-cell interaction systems. The results suggest a sequential series of events where activated MP cells secrete large amounts of fibronectin (FN), which triggers migration of pre-adipocytes out of mesenteric fat through integrin α5β1 signaling and promotes their differentiation into the mature adipocytes responsible for CF formation in CD.

METHODS

Isolation and culture of primary human intestinal cells

Procurement and histopathology of intestinal tissues and *Immunostaining* can be found in Supplementary Information. Primary human intestinal muscularis propria muscle cells (HIMC), and mesenteric pre-adipocytes were isolated from surgically resected intestinal specimen as previously described[11, 12] and kindly supported by Dr. Pothoulakis. To generate pre-adipocyte derived mesenteric adipocytes a previously described protocol[13] was used. A detailed description can be found in Supplementary Information, including Supplementary Figure 12.

Matrisome analysis of human intestinal muscularis propria muscle cell conditioned medium

Cell culture and induction of matrix production and *generation of the HIMC supernatants, size fractionation* and *immunoprecipitation* were conducted as described in Supplementary Information. For liquid chromatography mass spectrometry (LC-MS), HIMC conditioned medium in the presence of absence of TGF-β1 was used. Technical details can be found in Supplementary Information.

Wound healing assay of pre-adipocytes on human intestinal muscularis propria derived extracellular matrix

Two dimensional (2D) HIMC derived ECM scaffolds were generated and pre-adipocyes reseeded as described in detail in Supplementary Information, including Supplementary Figure 1.

Ex vivo model of human mesenteric fat outgrowth

An *ex vivo* human mesenteric fat tissue outgrowth model was prepared as previously described[14]. Briefly, fresh mesenteric fat tissue pieces were extensively washed with sterile HBSS with 2.5% PSF (Lonza) over 3 hours. Fat tissue was cut into 200mg wet weight pieces by sharp dissection and attached onto the HIMC derived ECM coated wells. Culture medium was added and the plate incubated at 37°C in 5 % CO_2 atmosphere. Medium was changed every 3 days. Cell outgrowth from the fat tissue was observed starting day 3 and migration traced using a Leica DMI6000 inverted microscope (Leica, Wetzlar, Germany).

Migration of pre-adipocytes on decellularized human intestine *ex vivo*

We first established decellularization of the human intestine as described previously[15]. Briefly, fresh full-thickness intestinal tissues were collected. Fat was removed from the tissue by sharp dissection before extensively rinsing it with PBS. Samples were cut into 5cm × 2cm pieces and incubated in sterile 1% sodium dodecyl sulfate (SDS; Fisher Scientific) in deionized water for 4–6 hours at room temperature with gentle shaking. Sterile 1% Triton-X100 (Sigma) in deionized water was applied to rinse the tissues for 1 hour and the acellular matrix was then washed in sterile PBS containing 2.5% PSF (Lonza) at 37°C for 5 days. The decellularized human intestinal matrix was stored at −80°C for up to 6 months. Molecular characterization was performed using H&E and Masson's Trichrome staining or immunofluorescence using specific antibodies to Col I (Rockland), Col III (Rockland), FN (Abcam) or DAPI (Invitrogen) (Supplementary Figure 2). Decellularized human intestinal tissue blocks were properly oriented and at the side of the MP, which was directly adjacent to the mesenteric fat, slices of 10μm thickness were generated, and placed on the plastic surface of wells of a 12-well cluster plate. Pre-adipocytes were stained with cell membrane lipophilic dye (PKH26, Sigma) and seeded onto the human intestinal decellularized matrix at a concentration of 200.000 cells/ml. After culture overnight, stained pre-adipocytes adherent to the decellularized MP ECM and cells were tracked using time-lapse microscopy as described. Quantitative analysis, including cell migration distance, displacement, velocity and directionality indices are described in Supplementary Information.

Immunofluorescence, Transfection of cell lines, Migration assay, Immunoblotting, Enzyme-linked immunosorbent assay, Flow cytometry analysis, Additionally used reagents and blocking antibodies, Statistics and *Ethical statement* can be found in Supplementary Information.

RESULTS

An inflammatory ECM scaffold is interposed between creeping fat and the muscularis propria in Crohn's disease

To explore whether the interaction between muscle cells and mesenteric fat leads to CF formation we investigated the spatial relationship of MP cells and CF by histopathology. CF was observed exclusively in CD-involved segments, but not NL, UC and uninvolved CD (Figure 1A)[16]. The CF leading edge was located *underneath* the serosa (Figure 1B), and an inflammatory ECM scaffold was positioned between CF and the MP (Figure 1C). The ECM scaffold contained abundant immune cells seemingly emanating from the transmural infiltrates of the MP cells (Figure 1C). Next, the thickness and area of the ECM scaffold in NL, UC, CD_{NS} and CD_S was assessed by sirius red staining of the mesenteric and anti-mesenteric side of the bowel (Figure 1D). Its thickness and area was markedly increased in CD_S compared to NL, UC and CD_{NS} bowel (Figure 1D&E), while on the anti-mesenteric side it was similar in all groups (Figure 1D), suggesting that only the CF adipocytes are exposed to the inflammatory ECM scaffold in CD_S.

Human intestinal muscularis propria muscle cells secrete a distinct matrisome

Since adipocytes are not considered a significant source of ECM proteins, MP cells emerge as a more likely source of ECM proteins forming the inflammatory scaffold in CD_S. To investigate the ECM protein secretory capacity of MP cells (HIMC) (instead of measuring preformed intracellular proteins or whole tissue lysates), we isolated HIMC from NL, UC, CD_{NS} and CD_S MP tissue (Supplemental Figures 3&4) incubated with and without the profibrotic factor TGF-β1[8, 17]. Supernatants of HIMC cultures were subjected to LC-MS[18], and results analyzed using standard proteomic analysis workflows (described in Methods). Proteins that passed quality control were interrogated for their presence in the matrisome[19], an omic inventory of ECM components and functions.

Principal component analysis (PCA) revealed no clustering differences in overall protein production among NL, UC, CD_{NS} and CD_S (data not shown). After TGF-β1 treatment an overlap between the matrisome produced by NL, UC and CD_{NS} HIMC was noted in treated versus untreated cells, and a clear separation was observed in CD_S (Figure 2A), suggesting a distinct cellular response of CD_S HIMC to TGF-β1. In fact, both the number and type of HIMC-derived ECM proteins were differentially expressed in NL, UC, CD_{NS} and CD_S after exposure to TGF-β1 as displayed in Venn diagrams, with TGF-β1 stimulated CD and CD_S HIMC producing unique ECM proteins (Figure 2B&C). The most significantly up or downregulated proteins were expressed in the CD_S compared to the CD_{NS} HIMC (Figure 2B&C).

A differential response of NL, UC, CD_{NS} and CD_S HIMC was noted in heatmap analysis, with clear up and downregulation of most ECM proteins depending on prior exposure or not to TGF-β1 (Figure 2D). Interestingly, diversity of the ECM proteins was not different between the groups in treated or untreated HIMC as determined by the Shannon index (Supplemental Figure 5). Based on the results of the heatmap analysis, we next focused on the top 25 most abundant ECM proteins in the HIMC supernatants.

Col IA1 and A2, decorin (DCN) and fibronectin (FN) were the top 4 most abundant proteins produced by NL, UC, CD_{NS} and CD_S HIMC (Figure 2E) but, after analyzing differences in protein abundance before and after TGF-β1 treatment (Supplemental Figure 6), only FN and DCN changed significantly but in opposite directions with FN being significantly upregulated and DCN significantly downregulated (Figure 2F).

Next, we looked for proteins that may be positively or negatively correlated to identify potential co-modulating protein pairs/groups. In untreated CDs HIMC, FN was significantly and positively correlated with LTBP2 and negatively correlated with COL18A1 and COL4A2 (Figure 2G). In contrast, in TGF-β1-treated CDs cells FN was positively correlated with COL6A2 and COLA3, and negatively correlated with COMP and COL4A2 (Figure 2G). Given that FN and DCN exhibit opposite functional properties[20] and concomitantly changed in opposite directions in response to TGF-β1 in our study, we focused on these two ECM molecules as key potential candidates for CF formation.

We performed immunofluorescence staining for FN, DCN, Col I and Col III in NL, UC, CD_{NS} and CD_S specifically focusing on the inflammatory ECM scaffold. In CD_S the

expression of FN was strikingly high, with that of DCN being barely visible, while the expression of FN and DCN in NL, UC and CD_{NS} tissues was variably low or moderate-to-high, respectively (Figure 2H). Of note, which the fat tissue itself only produced small amounts of FN, the thickened serosal layer was strongly positive, but without any communication with the ECM scaffold. In the same tissues, expression of Col I and III also varied from low to moderate with an increase in IBD tissues (Figure 2H). Next, we investigated expression of the same ECM proteins in HIMC monolayers in the absence or presence of TGF-β1. HIMC spontaneously expressed very low levels of FN, Col I, Col III, with a robust increase after exposure to TGF-β1 (Figure 2I), while DCN had a higher spontaneous expression in HIMC that, consistent with the proteomics findings, was markedly reduced after exposure to TGF-β1.

Preadipocytes migrate out of mesenteric fat onto muscle cell-derived ECM

To evaluate whether the inflammatory ECM scaffold participates in CF formation, we cultured NL HIMC to generate ECM *in vitro* to mimic the generation of the ECM scaffold *in vivo* (Figure 3A). While only occasional spindle-shaped cells migrated out of the mesenteric fat explants onto the uncoated plate at day 4 (Figure 3B, left panel), numerous cells migrated out of the fat explants onto the ECM-coated plate (Figure 3B, right panel). Not only the numbers of migrated cells was higher, but also the proportion of fat explants that generated migrating cells was higher in ECM-coated plates (Figure 3 B,C; Supplementary Material Video 1). Flow cytometric characterization of those migrated cells revealed them to be adipose mesenchymal stem cells (aMSC)[21] expressing preadipocyte factor 1 (Pref-1), which could be differentiated into mature adipocytes (Figure 3D to F; Detailed information in Supplementary Material).

HIMC derived ECM induces migration of mesenteric preadipocytes

The above results suggested that migration of pre-adipocytes out of mesenteric fat and their subsequent differentiation into adipocytes are events relevant to CF formation. To test this assumption, we investigated which HIMC-derived ECM components could induce pre-adipocytes migration, by using a Boyden chamber assay to verify migration towards HIMC-generated conditioned medium.

All pre-adipocytes derived from NL, UC, CD_{NS} and CD_S tissues migrated towards the same tissue-derived HIMC medium, a response robustly upregulated by TGF-β1 (Figure 4A). Similar results were obtained regardless of the origin of the pre-adipocytes and the HIMC medium. Interestingly pro-inflammatory factors like IL-1β or TNF-α, the growth factor b-FGF, or ligands specific for toll like receptors (TLR)2/6, TLR4, TLR5 and nucleotide-binding oligomerization domain (NOD)-1 failed to significantly increase pre-adipocyte migration (Figure 4A). When pre-adipocyte-derived adipocytes were tested in the same assays comparable results were obtained (Supplemental Figure 7A).

To identify the specific factors within HIMC-conditioned medium responsible for pre-adipocyte and adipocyte migration, HIMC conditioned medium was fractioned based on size. As shown in Figure 4B and Supplemental Figure 7B, migration was drastically reduced

after filtration through 30, 100 and 300 kDa pores, indicating that the molecular weight of the migration-inducing factors is large, compatible with the size of ECM components.

Fibronectin is the dominant migration-inducing factor in HIMC-conditioned medium

Given that the proteomic screen of HIMC-supernatants and HIMC IHC revealed FN, DCN and Col I and III to be the major components of the ECM scaffold, we individually tested these components for their capacity to promote pre-adipocytes and adipocyte migration, as well as growth factors (bFGF, TGF-β1), pro-inflammatory cytokines (TNF, IL-1β) and lipids (stearate, palmitate, oleate) (Figure 4C). Interestingly, only FN, Col I and Col III promoted migration, with FN inducing a dramatic dose-dependent 57-fold increase migration (Figure 4C). This is highly relevant because HIMC spontaneously secreted FN and its secretion is upregulated by TGF-β1 (Supplementary Figure 8A). To confirm that HIMC supernatant fractionation removed FN, no FN was detected in the filtered ECM supernatants (Supplemental Figure 8B). Since adipocytes and pre-adipocytes consistently showed similar behavior in all assays, and pre-adipocytes were the only cell type migrating out of fat explants, all subsequent experiments were performed with pre-adipocytes with some noted exceptions.

We next used immunoprecipitation to deplete HIMC supernatants of FN, which reduced migration by approximately 50% (Figure 4D, Supplementary Figure 8C), a decrease rescued by adding FN to FN-depleted supernatants (Figure 4D). Further evidence that FN is the dominant migration-inducing factor, its mRNA was knocked down with siRNA in HIMC (Supplementary Figure 8D) and supernatants were then generated from the same cells. Pre-adipocytes migrated significantly less towards these supernatants compared to supernatants from control HIMC (Figure 4E).

Given the differential expression of DCN in the matrisome analysis and its potentially overlapping signaling pathway with FN[22], we assessed pre-adipocyte migration in response to FN in the presence or absence of DCN, but found no changes in the presence or absence of this protein (Supplementary Figure 9). DCN also failed to influence migration of pre-adipocytes out of mesenteric fat when the assay was performed in FN-coated or uncoated plates (Supplementary Figure 10).

Fibronectin signaling mediates pre-adipocytes and adipocyte migration

After establishing that HIMC-produced FN is a major inducer of pre-adipocyte migration, we explored the signaling pathways involved. Integrins are critical sensors that mesenchymal cells use to communicate with the surrounding ECM milieu and are essential to mediate their migration[23]. Therefore, using HIMC supernatants, we pre-treated pre-adipocytes with GRGD to block the FN tripeptide Arg-Gly-Asp sequence which engages cell surface integrins. This strongly inhibited pre-adipocytes (Figure 4F) and adipocyte (Supplemental Figure 11) migration compared to the scrambled control GRAD (data not shown). Additionally, chemical blockade of focal adhesion kinase (FAK), a mediator downstream of integrins, also inhibited HIMC supernatant induced migration of pre-adipocytes and adipocytes (Figure 4F; Supplemental Figure 11).

Mesenteric preadipocytes express fibronectin binding integrins involved in migration

To identify which specific integrins were involved, we characterized the integrin expression on pre-adipocytes via flow cytometry by staining for integrin α1, 3, 5, V, IIb, 8 and β1, 3, 5, 6, 8[23]. Pre-adipocytes expressed integrins α3, α5, αv and β1, but not α1, αIIb, α8, β3, β5, β6 and β8. Intriguingly, the mean fluorescence intensity (MFI) of αv was significantly higher in CD_S compared to all other groups (Figure 5A&B).

To assess the functional relevance of the detected integrins we initially focused on integrin β1 because it is the central binding partner to the several other identified α subunits[23]. Antibody blockade of β1 resulted in a significantly decreased migration of pre-adipocytes towards NL, UC, CD_{NS} and CD_S in HIMC-conditioned medium regardless of previous HIMC exposure to TGF- β1 (Figure 6A). The apparent key role of integrin β1 in mediating migration was functionally confirmed in a wound healing assays (Figure 6B), where migration was substantially reduced by GRGD, FAK inhibition and integrin β1 blockade (Figure 6B&C).

To visualize and quantify migration of pre-adipocytes out of mesenteric fat we placed NL mesenteric fat explants onto HIMC-derived ECM and, using time lapse microscopy, we observed reduced distance, displacement, speed and persistence of pre-adipocytes when GRGD, integrin β1 antibody or a FAK inhibitor were added to the cultures (Figure 6D&E; Supplementary Material, Video 2). We also individually blocked the integrins α3 and α5 with antibodies and antagonists (GLPG0187 and CWHM-12) and noted that blockade of integrin α5 and αv, but not blockade of α3, reduced pre-adipocytes migration (Figure 7A).

To more closely examine the actual pre-adipocytes migration and physical interaction with ECM components we decellularized human intestinal tissue and developed a 3D ECM system (Figure 7B)[24], with preserved architecture and content as confirmed by H&E, MT, immunostaining, DNA analysis, absence of DAPI and RNA housekeeping genes, and retained protein expression compared to the original tissue (Supplementary Figure 2). We then obtained perpendicular frozen sections of the MP layer, placed the sections onto a culture dish, seeded them with fluorescently labelled pre-adipocytes, and performed live cell imaging in the presence or absence of integrins β1, α5 and αv inhibitors (Figure 7C&D; Supplementary Material, Video 3). In this 3D ECM system, a migration of pre-adipocytes along the ECM fibers was observed, and blockade of integrin β1 and α5, but not αv, reduced migration distance, displacement, speed and persistence (Figure 7D).

DISCUSSION

Increasing evidence suggests a previously unrecognized role of visceral fat in CD pathobiology and clinical manifestations. Increased visceral fat volume is an independent risk factor for disease recurrence after surgery[25], and rate of surgical recurrence decreases if mesenteric fat is removed [26]. CF is an exclusive feature of CD associated with complications and increased need of surgery[5]. These facts suggest that preventing or eliminating CF formation could represent a novel strategy to improve CD outcome and unravelling its mechanisms could lead to new forms of therapy. Therefore, we comprehensively investigated the potential mechanisms underlying CF formation by using

unique systems consisting of human intestinal muscle cells, pre-adipocytes, adipocytes, mesenteric fat explants and decellularized intestinal tissue. We identified MP cells, FN, integrin α5β1, and mesenteric fat pre-adipocytes as key players in the formation of CF in CD.

The direct anatomical apposition of CF with the MP implies functional communication between them[27]. So far, the interface between CF and the MP has not been investigated[5], but our results reveal an inter-positioned ECM scaffold between CF and the MP. ECM is acellular, however, it is not simply a physical structure, but a source of biochemical and biomechanical cues essential to tissue homeostasis[28]. We show that intestinal MP cells can produce a scaffold rich in multiple ECM molecules and capable of inducing the migration of pre-adipocytes out of mesenteric fat with subsequent capability to differentiate into mature adipocytes. The exact ECM secretory profile of HIMC has not been previously investigated, and we herein report the first comprehensive ECM matrisome from NL, UC, CD_{NS} and CD_S HIMC. Cells of all groups spontaneously secrete large amounts of ECM molecules with Col I, DCN and FN being the most abundant. This was not different between *untreated* strictured compared to non-strictured bowel HIMC. ECM however markedly increased after exposure to TGF-β1 in all groups, which is notable because TGF-β1 is elevated predominantly in strictured MP[29]. Qualitatively the FN secretion is not specific to CDs. However, its quantity is significantly increased in CDs due to the presence of a TGF-β1-rich microenvironment and as confirmed by our IF analysis in human tissues and hence can contribute to CF formation. These results represent a compelling reason to functionally explore ECM proteins in fibrostenotic CD. TGF-β1 downregulated DCN, a member of the proteoglycan family with anti-fibrotic properties [22]. This is relevant to CD_S since the balance of this dual but opposite effect obviously favors fibrogenesis at the expense of fibrosis resolution.

Directly relevant to the aims of this study is which ECM component most effectively induces migration of mesenteric adipocytes or pre-adipocytes involved in CF formation. We convincingly demonstrate that FN is that component[30], a finding consistent across cells from NL, UC, CD_{NS} and CD_S origin. The migration-inducing effect of FN is probably strengthened by the downregulation of DCN we found in CD_S tissue. In fact, DCN competes with FN for binding of integrin α5β1[22], but this is less likely here given low DCN expression, leaving FN free to bind α5β1 integrin on pre-adipocytes and promote their migration. In addition, DCN alone or in combination with FN neither induced nor suppressed pre-adipocyte migration.

While FN was more effective than Col I or Col III, no pro-inflammatory cytokine, growth factor or fatty acid was able to promote pre-adipocytes or adipocyte migration. This observation is important considering the presence of immune cells inside the CF ECM scaffold[28]. This is particularly intriguing in the case of TGF-β1. TGF-β1 activated MP muscle cell supernatants, which include all products these cells generate in response to TGF-β1, strongly induced pre-adipocyte migration. It is striking, however, that as shown in Figure 4C, TGF-β1 alone did not have any effect on pre-adipocyte or adipocyte migration. This indicates that TGF-β1 needs muscle cells to exert its indirect effect on pre-adipocytes. This also implies that inflammation and CF formation are mechanistically separate although

mutually dependent processes. At the same time, this by no means excludes potential crucial functional impacts of MP residing immune cells on the mesenteric or CF. In fact, the source of TGF-β1 comprises multiple different cell types[31], and immune cell released TGF-β1 may be a major driver of muscle cell activation. Integrins are essential for cell migration[23], but while little is known about their expression and function by adipocytes[32], no information exist about integrins in visceral fat pre-adipocytes. Given that FN induced pre-adipocyte migration, detailed integrin characterization and antibody blocking experiments concluded that integrin α5β1 is the major mediator of this function.

While informative, e*x vivo* systems have inherent limitations due to their two-dimensional nature and may or may not reflect ECM properties *in vivo*[15]. We hence recapitulated the mesenteric fat with MP interface by establishing and validating a decellularization protocol that created perpendicular sections of the outer MP, the area which is exposed to mesenteric fat. When placing pre-adipocytes onto this FN-rich ECM scaffold, we confirmed the importance of integrin α5β1 in pre-adipocyte migration. These experiments corroborate the integrin selectivity and function under circumstances that can be encountered *in vivo*.

Pre-adipocytes, the adipocyte precursor cells, display both migratory and proliferative activities, and during development they migrate into and form primitive fat organs as the initial step of physiological adipogenesis[33]. Thereafter, pre-adipocytes differentiate into mature adipocytes characterized by accumulation of lipid droplets[34]. These same events were observed in our experimental systems, where the cells that migrated out of mesenteric fat onto ECM were exclusively pre-adipocytes which subsequently differentiated into adipocytes upon encountering a FN-rich ECM. Pre-adipocytes also play a prominent role in pathological forms of adipogenesis, such as in obesity and diabetes, by contributing to the pool of adipocytes[35]. By combination of our results a scenario emerges in which pre-adipocytes are drawn out to mesenteric fat, migrate toward and attach to the HIMC-derived ECM scaffold and initiate CF formation (Supplementary Figure 13).

A limitation to the study of CF pathogenesis is the lack of *in viv*o experimental models of CF[36]. Nevertheless, our alternative models of *ex vivo* mesenteric fat explants and decellularized intestine do mimic *in vivo* phenomena occurring in CD patients, and bring novel therapeutic perspectives for CF prevention and, implicitly, for stricture formation in CD. For instance, selective blockade of pre-adipocytes migration, attachment, proliferation or differentiation could all be potential therapeutic strategies. Antibodies and molecules that modulate pathways we discovered already exist[37, 38], and have been tested experimentally in fibrotic diseases therapeutic trials (NCT02612051, NCT03573505, NCT03949530, NCT04072315). Our reported findings do not exclude other mechanisms contributing to CF formation, such as lymph contents or lymphatic angiogenesis[39]. In addition, other factors than TGF-β1, which was the focus of this investigation, may be capable of activating HIMC towards a phenotype that is able to attract pre-adipocytes and this is part of an ongoing project.

This study solely focused on the interaction of the MP relationship with pre-adipocytes and adipocytes, and multiple other tissue compartments, in particular immune cells, may have an influence on the formation and function of creeping CF. Of note, immune cells themselves

can express ECM genes, including FN[40, 41, 42], which suggests that the activated MP muscle cells may not be the only source of ECM in mesenteric fat and CF. Ongoing studies are assessing the impact of MP and fat residing immune cells on fat differentiation and fat fibrosis. Follow-up studies will likely identify additional targets for intervention thus enlarging the therapeutic armamentarium for fibrostenotic CD.

Supplementary Material

Refer to Web version on PubMed Central for supplementary material.

ACKNOWLEDGEMENTS

Abbreviations:

aMSC	adipose mesenchymal stem cell
BSA	Bovine serum albumin
CD	Crohn's disease
CEBPα	CCAAT/enhancer-binding protein
CF	Creeping fat
Col	Collagen
DMEM	Dulbecco's modified Eagle's medium
DTT	Dithiothreitol
E	Epithelial
ECM	Extracellular matrix
FABP4	Fatty acid-binding protein 4
FBS	Fetal bovine serum
FFPE	Formalin fixed paraffin embedded
FGF	Fibroblast growth factor
FN	Fibronectin
FAK	focal adhesion kinase
HBSS	Hank's Balanced Salt Solution
H&E	Hematoxylin & eosin

HIMC	Human intestinal muscularis propria muscle cells
IBD	Inflammatory bowel disease
IF	Immunofluorescence
IL	Interleukin
IBMX	3-Isobutyl-1-methylxanthine
LPS	Lipopolysaccharide
MEM	Minimum essential medium
MP	Muscularis propria
MT	Masson trichrome
NL	Normal
NOD	Nucleotide oligomerization domain
PAMP	Pathogen-associated molecular pattern
Pref-1	Preadipocyte factor 1
PSF	Penicillin, streptomycin, fungizone
siRNA	Small interfering RNA
SDS	Sodium dodecyl sulfate
SMA	Smooth muscle actin
TLR	Toll-like receptor
TNF	Tumor necrosis factor
UC	Ulcerative colitis

REFERENCES

1. Cosnes J, Nion-Larmurier I, Beaugerie L, et al. Impact of the increasing use of immunosuppressants in Crohn's disease on the need for intestinal surgery. Gut 2005;54:237–41. [PubMed: 15647188]

2. Thia KT, Sandborn WJ, Harmsen WS, et al. Risk factors associated with progression to intestinal complications of Crohn's disease in a population-based cohort. Gastroenterology 2010;139:1147–55. [PubMed: 20637205]

3. Rocha VZ, Libby P. Obesity, inflammation, and atherosclerosis. Nat Rev Cardiol 2009;6:399–409. [PubMed: 19399028]

4. Kredel LI, Siegmund B. Adipose-tissue and intestinal inflammation - visceral obesity and creeping fat. Front Immunol 2014;5:462. [PubMed: 25309544]

5. Mao R, Kurada S, Gordon IO, et al. The Mesenteric Fat and Intestinal Muscle Interface: Creeping Fat Influencing Stricture Formation in Crohn's Disease. Inflamm Bowel Dis 2019;25:421–6. [PubMed: 30346528]

6. Ha CWY, Martin A, Sepich-Poore GD, et al. Translocation of Viable Gut Microbiota to Mesenteric Adipose Drives Formation of Creeping Fat in Humans. Cell 2020.

7. Sheehan AL, Warren BF, Gear MW, et al. Fat-wrapping in Crohn's disease: pathological basis and relevance to surgical practice. Br J Surg 1992;79:955–8. [PubMed: 1422768]

8. Severi C, Sferra R, Scirocco A, et al. Contribution of intestinal smooth muscle to Crohn's disease fibrogenesis. Eur J Histochem 2014;58:2457. [PubMed: 25578979]

9. Gordon IO, Bettenworth D, Bokemeyer A, et al. Histopathology Scoring Systems of Stenosis Associated With Small Bowel Crohn's Disease: A Systematic Review. Gastroenterology 2019.

10. Crohn BB, Ginzburg L, Oppenheimer GD. Landmark article Oct 15, 1932. Regional ileitis. A pathological and clinical entity. By Burril B. Crohn, Leon Ginzburg, and Gordon D Oppenheimer. JAMA 1984;251:73–9. [PubMed: 6361290]

11. Rieder F, Nonevski I, Ma J, et al. T-helper 2 cytokines, transforming growth factor beta1, and eosinophil products induce fibrogenesis and alter muscle motility in patients with eosinophilic esophagitis. Gastroenterology 2014;146:1266–77 e1–9. [PubMed: 24486052]

12. Sideri A, Bakirtzi K, Shih DQ, et al. Substance P mediates pro-inflammatory cytokine release form mesenteric adipocytes in Inflammatory Bowel Disease patients. Cell Mol Gastroenterol Hepatol 2015;1:420–32. [PubMed: 26543894]

13. Lee MJ, Fried SK. Glucocorticoids antagonize tumor necrosis factor-alpha-stimulated lipolysis and resistance to the antilipolytic effect of insulin in human adipocytes. Am J Physiol Endocrinol Metab 2012;303:E1126–33. [PubMed: 22949029]

14. Jing W, Xiao J, Xiong Z, et al. Explant culture: an efficient method to isolate adipose-derived stromal cells for tissue engineering. Artif Organs 2011;35:105–12. [PubMed: 20946305]

15. Chen HJ, Wei Z, Sun J, et al. A recellularized human colon model identifies cancer driver genes. Nat Biotechnol 2016;34:845–51. [PubMed: 27398792]

16. Shelley-Fraser G, Borley NR, Warren BF, et al. The connective tissue changes of Crohn's disease. Histopathology 2012;60:1034–44. [PubMed: 22008086]

17. Li C, Iness A, Yoon J, et al. Noncanonical STAT3 activation regulates excess TGF-beta1 and collagen I expression in muscle of stricturing Crohn's disease. J Immunol 2015;194:3422–31. [PubMed: 25740948]

18. Arif A, Jia J, Willard B, et al. Multisite Phosphorylation of S6K1 Directs a Kinase Phospho-code that Determines Substrate Selection. Mol Cell 2019;73:446–57 e6. [PubMed: 30612880]

19. Naba A, Clauser KR, Hoersch S, et al. The matrisome: in silico definition and in vivo characterization by proteomics of normal and tumor extracellular matrices. Mol Cell Proteomics 2012;11:M111 014647.

20. Goetsch KP, Niesler CU. The extracellular matrix regulates the effect of decorin and transforming growth factor beta-2 (TGF-beta2) on myoblast migration. Biochem Biophys Res Commun 2016;479:351–7. [PubMed: 27644884]

21. Dominici M, Le Blanc K, Mueller I, et al. Minimal criteria for defining multipotent mesenchymal stromal cells. The International Society for Cellular Therapy position statement. Cytotherapy 2006;8:315–7. [PubMed: 16923606]

22. Kennelly TM, Li Y, Cao Y, et al. Distinct Binding Interactions of alpha5beta1-Integrin and Proteoglycans with Fibronectin. Biophys J 2019;117:688–95. [PubMed: 31337547]

23. Johansson S, Svineng G, Wennerberg K, et al. Fibronectin-integrin interactions. Front Biosci 1997;2:d126–46. [PubMed: 9159220]

24. Lin S, Mao R, Wang J, et al. Successful Establishment of Decellularized Intestinal Extracellular Matrix 3D Scaffolds with Preserved Structure, Components and Function. Gastroenterology 2020;158:S–1042.

25. Li Y, Zhu W, Gong J, et al. Visceral fat area is associated with a high risk for early postoperative recurrence in Crohn's disease. Colorectal Dis 2015;17:225–34. [PubMed: 25307174]

26. Coffey CJ, Kiernan MG, Sahebally SM, et al. Inclusion of the Mesentery in Ileocolic Resection for Crohn's Disease is Associated With Reduced Surgical Recurrence. Journal of Crohn's & colitis 2018;12:1139–50.

27. Coffey JC, O'Leary D P. Defining the mesentery as an organ and what this means for understanding its roles in digestive disorders. Expert Rev Gastroenterol Hepatol 2017;11:703–5. [PubMed: 28482706]

28. Rieder F, Fiocchi C, Rogler G. Mechanisms, Management, and Treatment of Fibrosis in Patients With Inflammatory Bowel Diseases. Gastroenterology 2017;152:340–50 e6. [PubMed: 27720839]

29. Graham MF, Diegelmann RF, Elson CO, et al. Collagen content and types in the intestinal strictures of Crohn's disease. Gastroenterology 1988;94:257–65. [PubMed: 3335305]

30. Leeb SN, Vogl D, Grossmann J, et al. Autocrine fibronectin-induced migration of human colonic fibroblasts. Am J Gastroenterol 2004;99:335–40. [PubMed: 15046226]

31. Branton MH, Kopp JB. TGF-beta and fibrosis. Microbes Infect 1999;1:1349–65. [PubMed: 10611762]

32. Ruiz-Ojeda FJ, Mendez-Gutierrez A, Aguilera CM, et al. Extracellular Matrix Remodeling of Adipose Tissue in Obesity and Metabolic Diseases. Int J Mol Sci 2019;20.

33. Crandall DL, Busler DE, McHendry-Rinde B, et al. Autocrine regulation of human preadipocyte migration by plasminogen activator inhibitor-1. J Clin Endocrinol Metab 2000;85:2609–14. [PubMed: 10902815]

34. Billon N, Iannarelli P, Monteiro MC, et al. The generation of adipocytes by the neural crest. Development 2007;134:2283–92. [PubMed: 17507398]

35. Isakson P, Hammarstedt A, Gustafson B, et al. Impaired preadipocyte differentiation in human abdominal obesity: role of Wnt, tumor necrosis factor-alpha, and inflammation. Diabetes 2009;58:1550–7. [PubMed: 19351711]

36. Rieder F, Kessler S, Sans M, et al. Animal models of intestinal fibrosis: new tools for the understanding of pathogenesis and therapy of human disease. Am J Physiol Gastrointest Liver Physiol 2012;303:G786–801. [PubMed: 22878121]

37. Maden CH, Fairman D, Chalker M, et al. Safety, tolerability and pharmacokinetics of GSK3008348, a novel integrin alphavbeta6 inhibitor, in healthy participants. Eur J Clin Pharmacol 2018;74:701–9. [PubMed: 29532104]

38. Reed NI, Jo H, Chen C, et al. The alphavbeta1 integrin plays a critical in vivo role in tissue fibrosis. Sci Transl Med 2015;7:288ra79.

39. Kuan EL, Ivanov S, Bridenbaugh EA, et al. Collecting lymphatic vessel permeability facilitates adipose tissue inflammation and distribution of antigen to lymph node-homing adipose tissue dendritic cells. J Immunol 2015;194:5200–10. [PubMed: 25917096]

40. Li Z, Zhang Y, Liu Z, et al. ECM1 controls T(H)2 cell egress from lymph nodes through re-expression of S1P(1). Nat Immunol 2011;12:178–85. [PubMed: 21217760]

41. Zhang Y, Li X, Luo Z, et al. ECM1 is an essential factor for the determination of M1 macrophage polarization in IBD in response to LPS stimulation. Proc Natl Acad Sci U S A 2020;117:3083–92. [PubMed: 31980528]

42. Efthymiou G, Saint A, Ruff M, et al. Shaping Up the Tumor Microenvironment With Cellular Fibronectin. Front Oncol 2020;10:641. [PubMed: 32426283]

WHAT YOU NEED TO KNOW

**What is already known about this subject?**

Creeping fat is a distinctive feature of Crohn's disease linked to strictures, luminal narrowing and bowel obstruction. Understanding its pathogenesis may lead to novel ways to prevent or eliminate stricture formation.

What are the new findings?

Activated muscularis propria muscle cells secrete a distinct matrisome, with increased amounts of the ECM component fibronectin which, through an integrin α5β1-mediated signaling, induces migration of pre-adipocytes out of mesenteric fat and *de novo* formation of creeping fat.

How might it impact on clinical practice in the foreseeable future?

This study comprehensively investigates the mechanisms of creeping fat formation in Crohn's disease. Inhibiting creeping fat formation may prevent or treat Crohn's disease associated complications in the future.
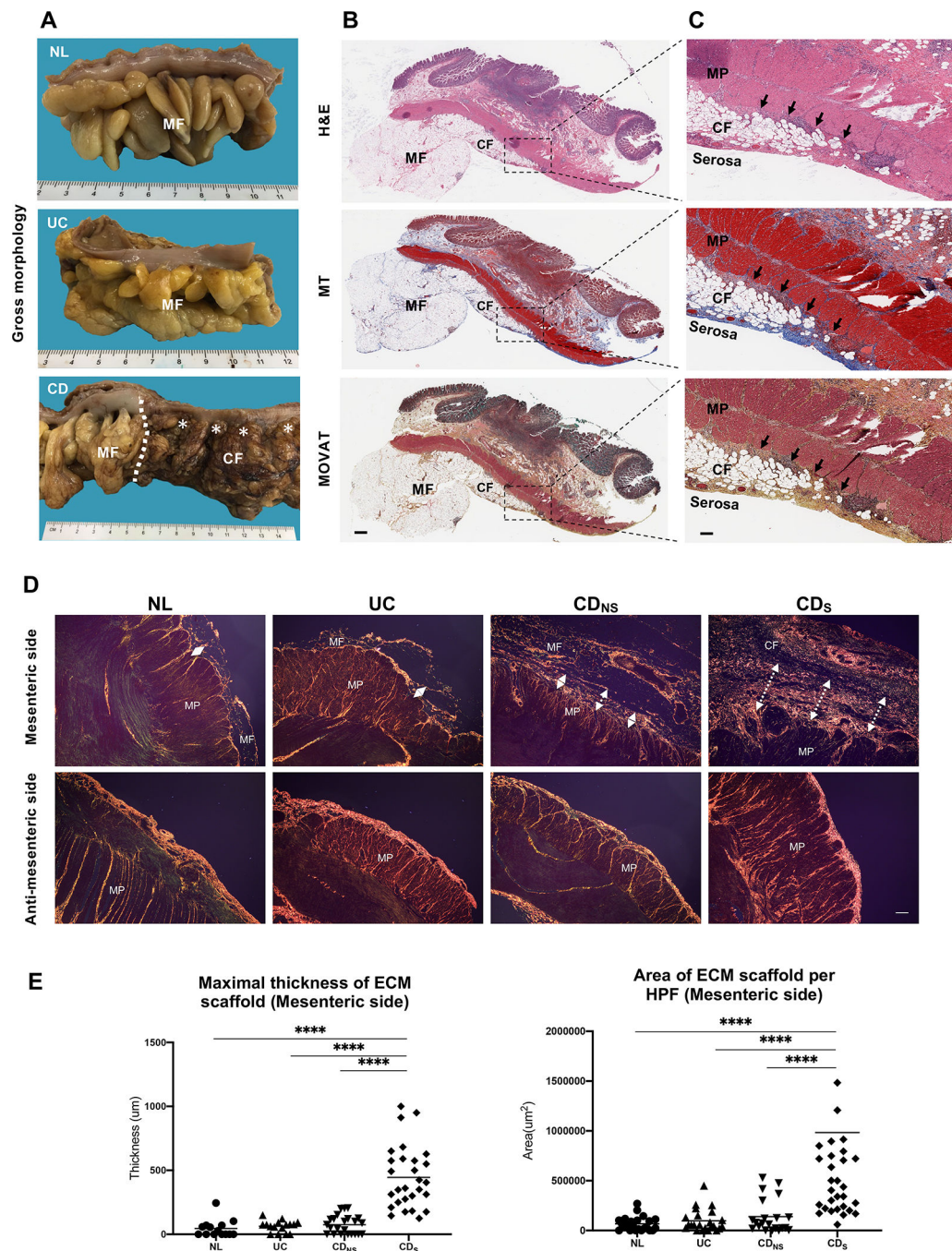
Figure 1. Histopathology evaluation of human intestinal resections for creeping fat

(**A**) Gross pathology appearance of normal colon (NL) with mesenteric fat, ulcerative colitis (UC) with mesenteric fat (MF), Crohn's disease (CD) with creeping fat (CF) on the right and normal MF on the left of the transition zone (dotted line). Pictures representative of n=7 in each group.

(**B**) CD tissue with MF and subserosal CF stained with H&E, MT and MOVAT. Pictures representative of n=5 in each group. Magnification 3X. Scale bar: 1mm.

(**C**) Closeup of panel B showing CF inter-positioned between the serosa and the MP in CD and a matrix scaffold (arrows) between the outer circular layer of the MP and CF (20X). Scale bar: 200μm.

(**D**) Sirius red staining of the mesenteric and anti-mesenteric side of the colon showing a thicker ECM scaffold in CD_S with CF compared to CD_{NS}, UC and NL. Magnification 40X. Scale bar 100μm.

(**E**) Thickness and area of the ECM scaffold are significantly increased in CD_S compared to CD_{NS}, UC and NL. One plot symbol represents one measurement in one patient. N=20–29 subjects per group.

Abbreviations: CD_{NS}, non-strictured CD; CD_S, strictured CD; Mesenteric fat: MF; Creeping fat: CF; Muscularis propria: MP; H&E, hematoxylin & eosin; MT, Masson Trichrome: MT; MOVAT, Movat Pentachrome; ECM, extracellular matrix; HPF, high power field; ****= p<0.0001.
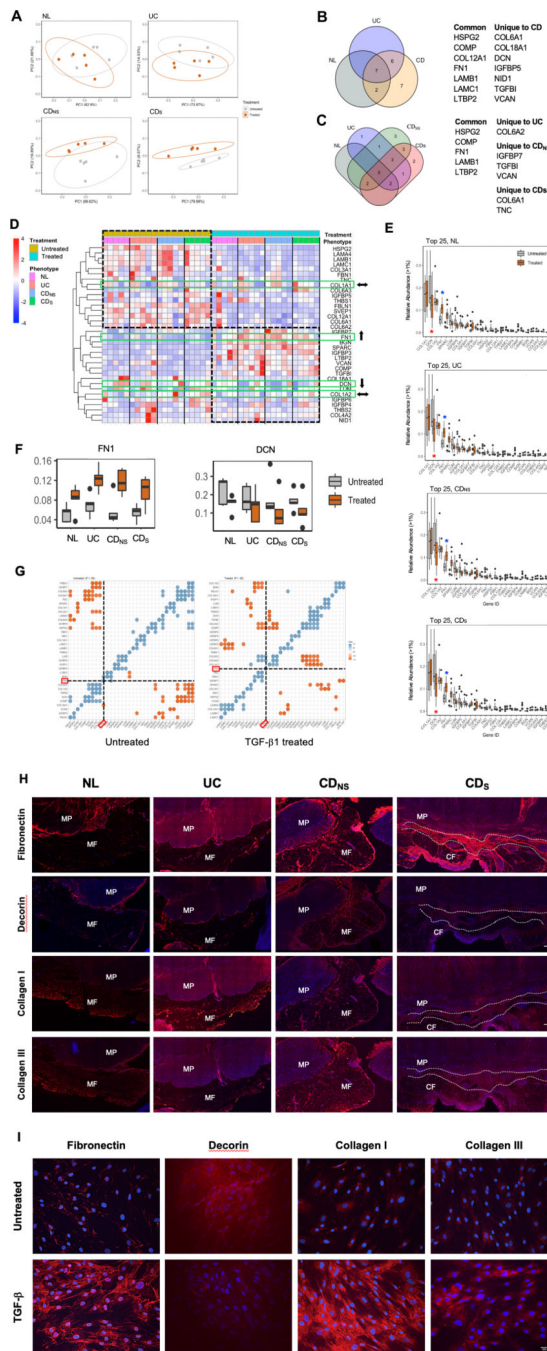
Figure 2. Mass spectrometry analysis of extracellular matrix proteins in supernatants from HIMC cultures of different phenotypes

(**A**) Principal components analysis of the relative abundance of matrisome proteins produced by NL, UC, CD$_{NS}$ and CDs; Ellipses indicate 95% confidence intervals. Separation of the matrisome components was noted in CD$_S$ between untreated and TGF-β1 exposure group. NL, UC, CD$_{NS}$ did not exhibit matrisome changes.

(**B and C**) Significantly different ECM proteins produced by NL, UC, CD$_{NS}$, and CDs HIMC exposed to TGF-β1. Proteins produced by treated and untreated HIMC were

quantified and compared, and Venn diagrams were created using only the proteins that were significantly different between the treated and untreated groups among the four phenotypes. (**B**) seven proteins were produced by all HIMC, but seven were produced exclusively by CD HIMC, six were shared between CD and UC, and 2 between CD and NL. (**C**): when protein production by CD HIMC was analyzed based on the cell origin from non-strictured or strictured tissue, three were produced by non-strictured and two by strictured HIMC.

(**D**) Unsupervised hierarchical clustering of ECM proteins (normalized relative abundance) produced by TGF-β-treated -untreated HIMC. Overall decreased and increased protein abundance was observed in most ECM proteins upon TGF-β exposure regardless of the NL, UC or CD phenotype of the cells. When the four most abundant ECM protein (Figure 2E) were individually analyzed (green rectangles), COL1A1 and COL1A2 remained essentially unchanged (⬌) regardless of cell phenotype, while FN1 clearly increased (⬆ □) and DCN decreased (⬇ □).

(**E**) Top 25 ECM proteins produced by HIMC ranked by level of abundance and degree of change according to TGF-β-treated or -untreated status. While in all HIMC phenotypes COL1A1 and COL1A2 abundance remained essentially unchanged, FN1 was the most upregulated (red asterisk) and DCN the most downregulated (blue asterisk) ECM protein.

(**F**) Box plots showing relative abundance of FN1 in TGF-β-treated and -untreated HIMC from the NL, UC, CD_{NS} and CDs phenotypes. Levels of FN1 significantly increased in HIMC from all HIMC phenotypes, while levels of DCN were decreased (P .05 for all comparisons). (n=20)

(**G**) Correlograms showing statistically significant correlations between ECM proteins in TGF-β-treated and -untreated HIMC from CDs (Spearman correlation, P .05). In untreated cells, FN1 was positively correlated with BGN and LTBP2, and negatively correlated with COL18A1, while in TGF-β–treated cells, FN1 was positively correlated with COL6A2 and COL6A3, and negatively correlated with COMP and COL4A2. Blue dots indicate positive correlation and brown dots indicate negative correlation.

H) Representative immunofluorescence staining of fibronectin, collagen I, collagen III and decorin at the interface between muscularis propria and mesenteric fat in NL, UC and non-strictured CD and creeping fat in strictured CD tissues. NL, normal; UC, ulcerative colitis; CD_{NS}, non-strictured Crohn's disease; CD_S, strictured Crohn's disease; MF, mesenteric fat; CF, creeping fat; MP, muscularis propria. Scale bar: 200μm. Slides are representative of n=3 per group.

(**I**) Immunofluorescence staining of fibronectin, collagen I, collagen III and decorin (red) and DAPI (blue) in TGF-β-treated and -untreated NL HIMC Scale bar: 100μm. Slides are representative of n=4 per group.
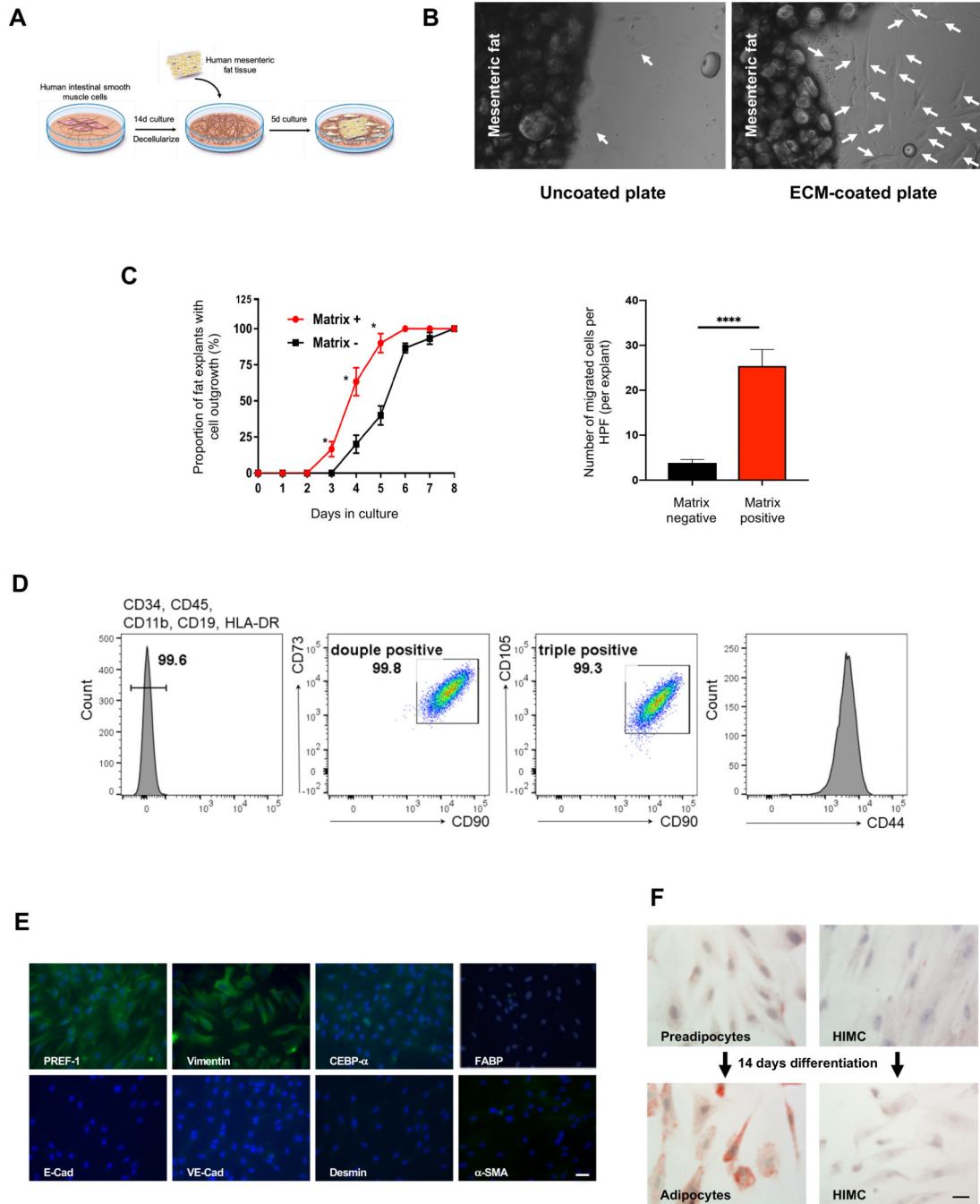
Figure 3. Human mesenteric fat ex vivo cell outgrowth model.

(**A**) Layout of human mesenteric fat *ex vivo* cell outgrowth on HIMC-derived ECM.
(**B**) Representative images of cell outgrowth (arrows) from normal mesenteric fat tissue plated on plastic (left) or HIMC-derived ECM (right) (phase contrast images at day 5 of culture) (n=3 independent experiments with 4–6 fat pieces each). A representative video can be found in Supplemental Material (Video 1).

(**C**) Differential, time-dependent outgrowth of cells outgrown from human mesenteric fat tissue plated on plastic alone (Matrix -) or HIMC-derived ECM (Matrix+). *P<0.05, ****P<0.001. (n=3 independent experiments with 4–6 fat pieces each).

(**D**) Phenotype of human mesenteric fat-outgrown cells showing >99% positivity for CD90, CD73 and CD105, and no expression of CD34, CD11b, CD19, CD45 or HLA-DR. Flow cytometry results representative of 3–5 experiments.

(**E**) Immunofluorescence staining for preadipocyte factor 1 (Pref-1), vimentin, CCAAT/ enhancer-binding protein (CEBPα), fatty acid-binding protein 4 (FABP4), E-cadherin, VE-cadherin, desmin and α-SMA in cells outgrown from human mesenteric fat tissue. Figure representative of 3–5 experiments. Scalebar 100μm.

(**F**) Acquisition of oil-red-O positivity by pre-adipocytes, but not human intestinal muscle cells (HIMC), upon differentiation into mature adipocytes after 14 days in culture. Figure representative of 3–5experiments. Scalebar 100μm.
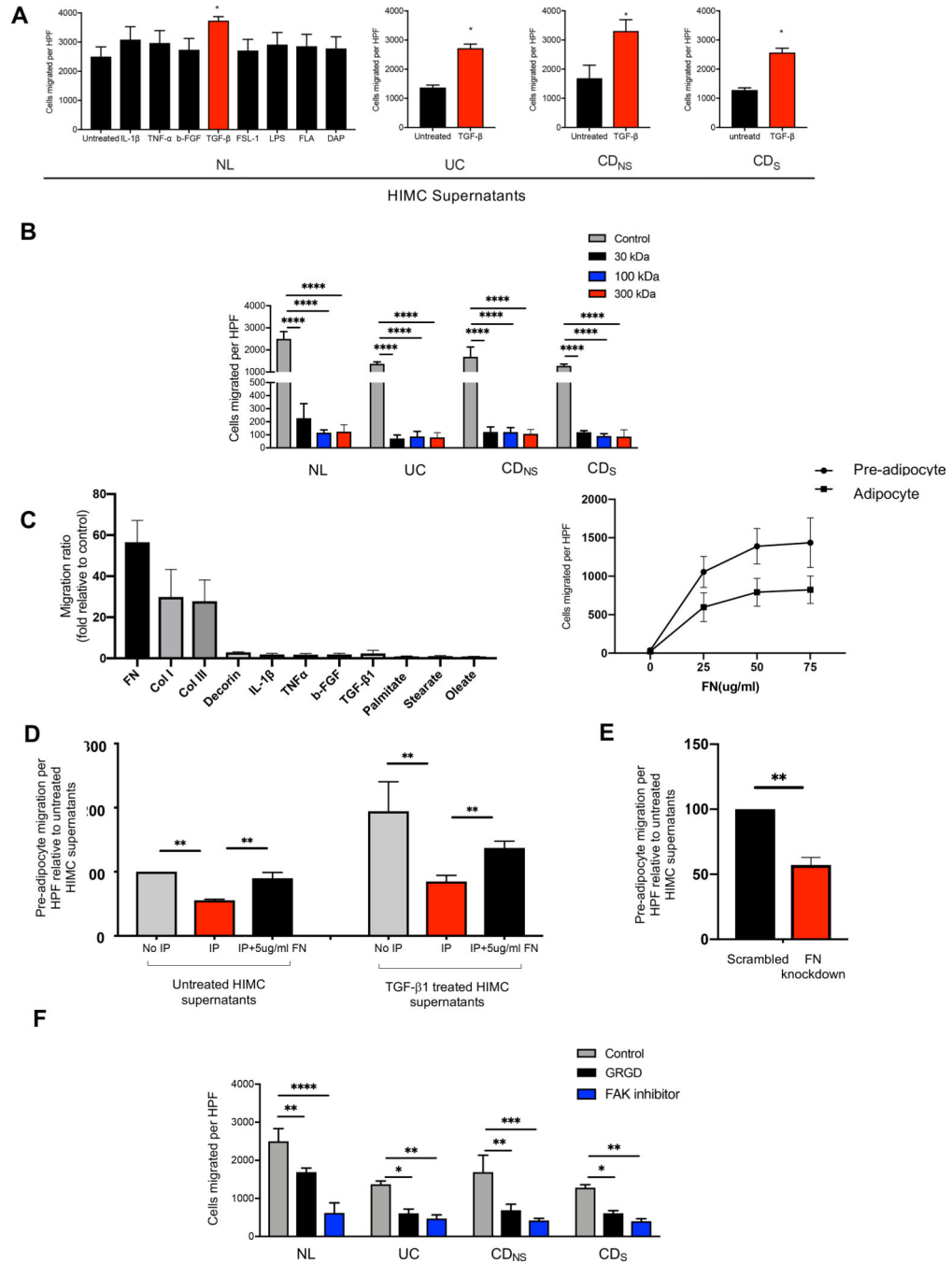
Figure 4. Fibronectin in HIMC conditioned medium is responsible for pre-adipocyte migration

(**A**) Migration of pre-adipocytes in the Boyden chamber is significantly increased by conditioned medium of NL, UC, CD$_{NS}$ and CD$_S$ HIMC exposed to TGF-β1 but not to pro-inflammatory cytokines (IL-1β, TNF-α), growth factor (b-FGF) or PAMP ligands. *P<0.05. (n=4–6)

(**B**) Filtration of HIMC conditioned medium through a 30, 100 and 300 KDa pore size significantly reduces migration of pre-adipocytes in the Boyden chamber. ****P<0.0001. (n=4–6)

(**C**) <u>Left</u>: Fibronectin has the strongest effect on inducing migration of pre-adipocytes compared with other ECM proteins (Collagen I, collagen III, decorin), cytokines ((IL-1β, TNF-a), growth factor (b-FGF) and fatty acids (palmitate, stearate, oleate). <u>Right</u>: Fibronectin-induced migration of pre-adipocytes and adipocytes in a dose-dependent manner. (n=3–5)

(**D**) Removal of fibronectin from HIMC-conditioned medium by immunoprecipitation significantly (**=P<0.01) reduces migration of pre-adipocytes in the Boyden chamber, while addition of soluble fibronectin to the fibronectin-depleted conditioned medium restores migration

(**E**) Removal of fibronectin from HIMC by siRNA knockdown reduces migration of pre-adipocytes in the Boyden chamber (**=P<0.01)

(**F**) Inhibition of HIMC-conditioned medium-induced pre-adipocyte migration in the Boyden chamber by GRGD and a focal adhesion kinase (FAK) inhibitor. (n=4–6)

Abbreviations: Normal: NL; Ulcerative colitis: UC; Crohn's disease: CD; CD_{NS}: non-strictured; CD_S: strictured; Fibronectin: FN; Collagen: Col; Immunoprecipitation: IP; Human intestinal muscularis propria smooth muscle cells: HIMC; Transforming growth factor: TGF

A

B
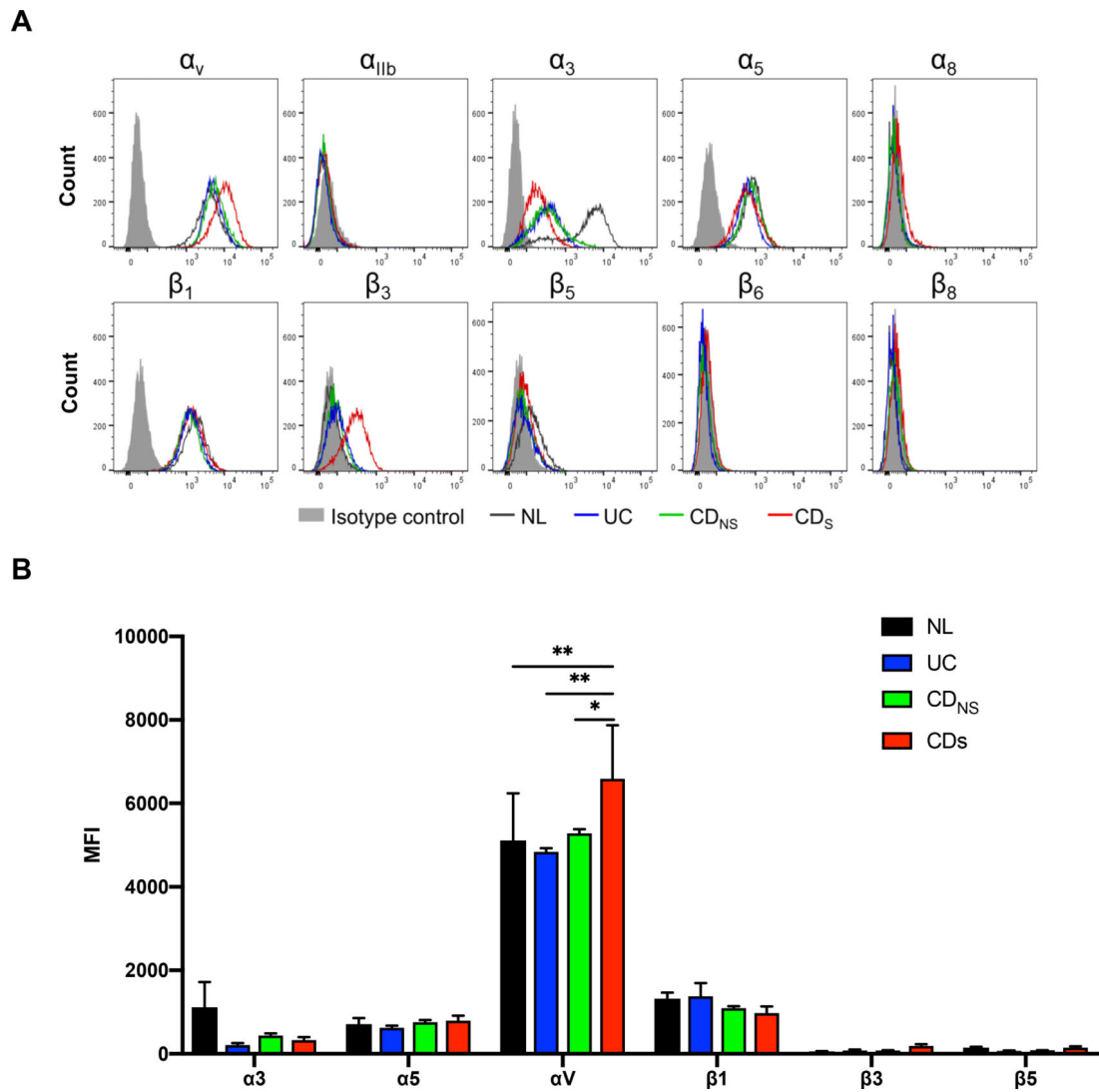
Figure 5. Integrin profiles of pre-adipocytes migrated out of mesenteric fat

(**A**) Flow cytometry analysis demonstrating that pre-adipocytes from CD_S, CD_{NS}, UC and NL expressed integrins $\alpha 3$, $\alpha 5$, αv and $\beta 1$, but not $\alpha 1$, αIIb, $\alpha 8$, $\beta 3$, $\beta 5$, $\beta 6$ and $\beta 8$. (n=5)

(**B**) Mean fluorescence intensity showing a higher expression of αv in CD_S compared to NL, UC and CD_{NS}. (n=5)

NL, Normal; UC, ulcerative colitis; CD, Crohn's disease; CD_{NS}: non-strictured Crohn's disease; CD_S: strictured Crohn's disease. MFI, mean fluorescence intensity. *P<0.05, **P<0.01.
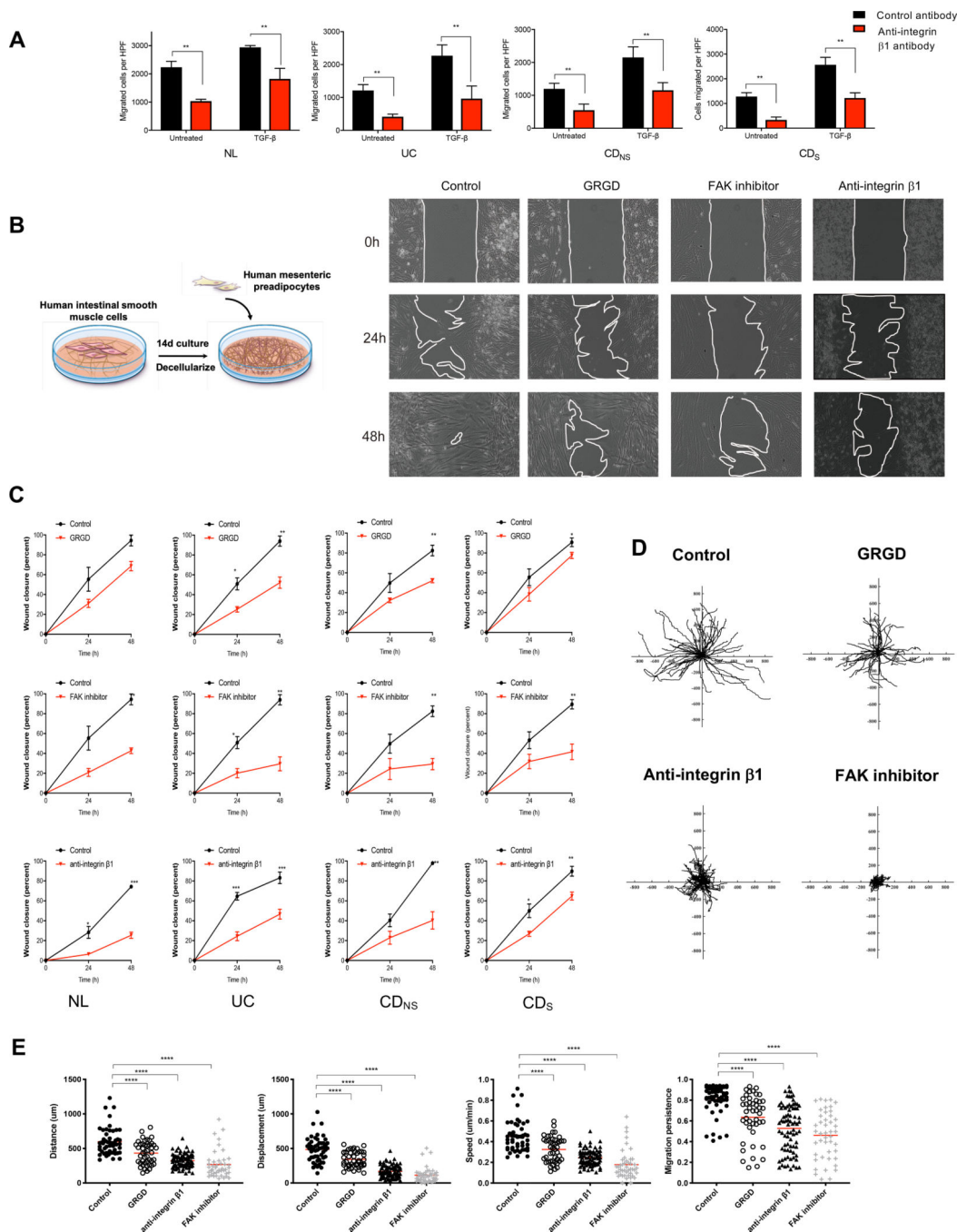
Figure 6. Integrin β1 regulates pre-adipocyte migration on HIMC-derived extracellular matrix
(**A**) Blockade of integrin β1 significantly reduces migration of NL, UC, CD$_{NS}$ and CD$_S$ pre-adipocytes towards HIMC-conditioned medium in the Boyden chamber irrespective of the presence of TGF-β1. **P<0.01. (n=4–5)

(**B**) Left: Layout of wound healing assay of pre-adipocyte migration on HIMC-derived ECM. Right: Representative phase contrast images of wound closure by pre-adipocyte migration at baseline, 24h and 48h, and effect of GRGD, FAK inhibition and integrin β1 blockade on migration. (n=4–5).

(**C**) Wound closure was inhibited by GRGD, integrin β1 blocking antibody and FAK inhibitor for NL, UC, CD$_{NS}$ and CD$_S$ preadipocytes. (n=4–5).

(**D**) Representative tracking of pre-adipocytes seeded on HIMC-derived ECM was performed for 24h in the absence (control) and presence of GRGD, integrin β1 blocking antibody and FAK inhibitor. (n=4–5). A representative video can be found in the supplement (Video 2).

(**E**) Distance, displacement, velocity and migration persistence of pre-adipocyte migration on HIMC-derived ECM in untreated and following addition of GRGD, blocking antibodies to integrin β1 and FAK inhibitor. (n=4–5 with tracking n>50 cells per condition).

NL, Normal; UC, ulcerative colitis; CD, Crohn's disease; CD$_{NS}$: non-strictured Crohn's disease; CD$_S$: strictured Crohn's disease. Focal adhesion kinase: FAK; statistically significant data are indicated by *P<0.05, **P<0.01, ***P<0.001,****P<0.0001.
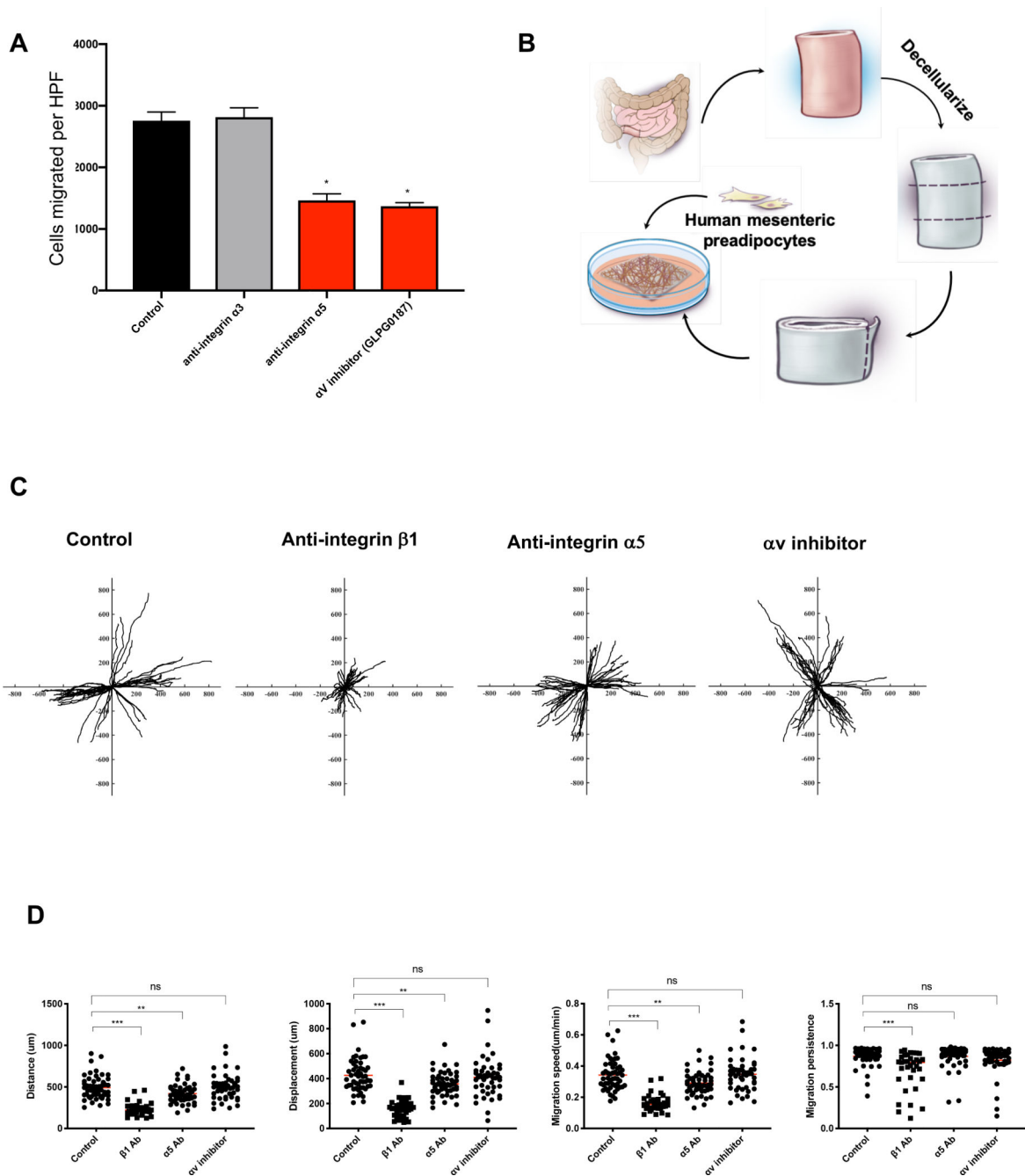
Figure 7. Integrin α5β1 regulates pre-adipocyte migration on the decellularized muscularis propria layer of human intestine.

(**A**) Integrin α5 blocking antibody and GLPG0187 (integrin αv antagonist) but not α3 blocking antibody reduced the migration of pre-adipocytes towards HIMC conditioned medium in the Boyden chamber. (n=5)

(**B**) Schema of experimental set-up for the decellularized human intestinal muscularis propria experiments.

(**C**) Representative tracking of pre-adipocytes seeded on decellularized human muscularis propria was performed for 24 h in the absence (control) and presence of integrin β1 blocking

antibody, α5 blocking antibody, and GLPG0187 (integrin αv antagonist). Representative video can be found in the supplement (Video 3).

(**D**) Distance, displacement, velocity and migration persistence of pre-adipocytes migration on decellularized human intestine with adding integrin β1 and α5 blocking antibody, and GLPG0187 (integrin αv antagonist). n=4 for decellularized muscularis propria. One symbol represents one tracked pre-adipocyte. Abbreviations: Antibody: Ab; Statistically significant data are indicated by *=P<0.05, **=P<0.01, ***=P<0.001.